Effects of Ground Failure on Bridges, Roads, and Railroads

Christian Ledezma,[a] Tara Hutchinson,[b] M.EERI, Scott A. Ashford,[c] M.EERI, Robb Moss,[d] M.EERI, Pedro Arduino,[e] Jonathan D. Bray,[f] M.EERI, Scott Olson,[h] M.EERI, Youssef M.A. Hashash,[h] M.EERI, Ramón Verdugo,[j] David Frost,[i] M.EERI, Robert Kayen,[g] M.EERI, and Kyle Rollins,[k] M.EERI

The long duration and strong velocity content of the motions produced by the 27 February 2010 Maule earthquake resulted in widespread liquefaction and lateral spreading in several urban and other regions of Chile. In particular, critical lifeline structures such as bridges, roadway embankments, and railroads were damaged by ground shaking and ground failure. This paper describes the effects that ground failure had on a number of bridges, roadway embankments, and railroads during this major earthquake. [DOI: 10.1193/1.4000024]

INTRODUCTION

The 27 February 2010 moment magnitude 8.8 Maule earthquake triggered liquefaction over a large area of Chile, particularly near rivers, streams, and along the coastline of the country. The widespread alluvial sediments and long duration of shaking most likely contributed to the large number of observations of liquefaction. Based on strong motion records processed to date, ground shaking in the Santiago area lasted for more than two minutes. Long-duration events subject loose, saturated, granular soils to a significant number of strain cycles and an associated generation of excess pore pressure. Liquefaction was observed in areas as far north as Viña Del Mar and Valparaíso, and as far south as Arauco and Lebu. Observations of liquefaction are bounded by the area just east of the Pan American highway. Figure 1 shows localities and spatial distribution of liquefaction occurrences. Field inspections carried out after the earthquake showed clear evidence of liquefaction at several locations as indicated in Figure 1a. The sites where liquefaction was observed correspond, approximately, to areas with Modified Mercalli intensities, as estimated by the U.S. Geological Survey (USGS 2010), larger than V to VI (Figure 1b).

[a] Pontificia Universidad Católica de Chile, Vicuña Mackenna 4860, Macul, Santiago, Chile
[b] University of California, San Diego, 9500 Gilman Drive, MC 0085, La Jolla, CA 92093-0085
[c] Oregon State University, 220 Owen Hall, Corvallis, OR 97331-3212
[d] California Polytechnic State University, San Luis Obispo, CA 93407
[e] University of Washington, Seattle, WA 98195-2700
[f] University of California, Berkeley, 453 Davis Hall, Berkeley, CA 94720-1710
[g] U.S. Geological Survey, 345 Middlefield Road MS 999, Menlo Park, CA 94025
[h] University of Illinois at Urbana-Champaign, 205 N. Mathews Ave. Urbana, IL 61801
[i] Georgia Institute of Technology, 790 Atlantic Drive, GeorgiaTech, Atlanta, GA 30332-0355
[j] Universidad de Chile, Departamento de Ingeniería Civil, Av. Blanco Encalada 2002, Santiago, Chile
[k] Brigham Young University, 368 CB, Provo, UT 84602

Earthquake Spectra, Volume 28, No. S1, pages S119–S143, June 2012; © 2012, Earthquake Engineering Research Institute

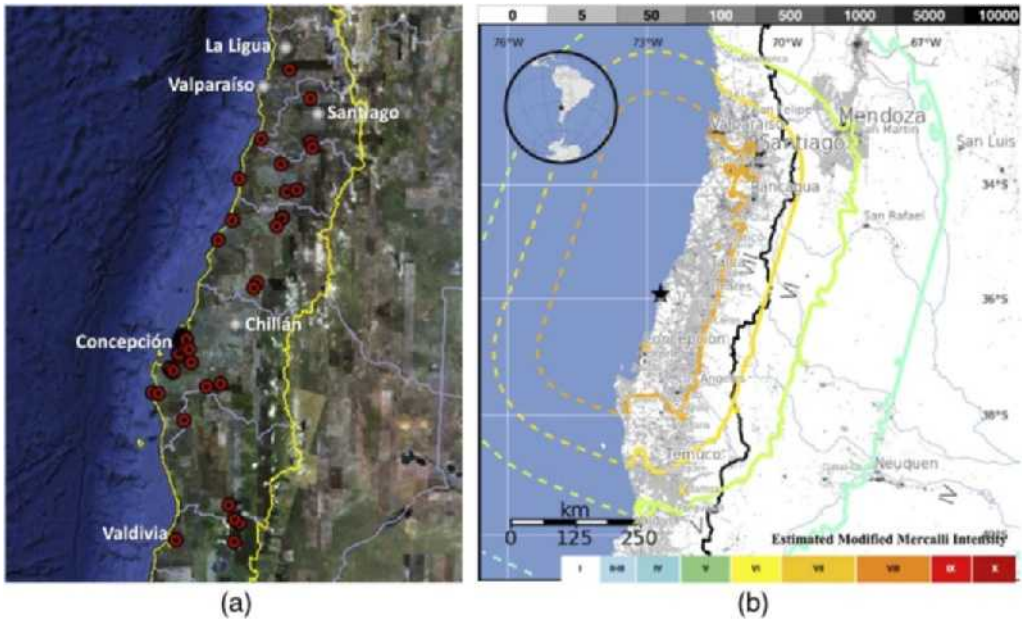

Figure 1. Spatial distribution of observed liquefaction, where surface evidence of liquefaction included ejected sand and lateral spreads: (a) Sites where liquefaction was observed (Verdugo 2011) and (b) Modified Mercalli Intensity map (USGS 2010).

Besides key factors responsible for liquefaction occurrence, such as the intensity and duration of the ground motion, and the relative density of granular soils, particle size and distribution could also have played an important role in the occurrence of liquefaction in this event. As the rivers travel from east to west, the slope and therefore the available energy for transporting particles decreases. The rivers begin on the steep flanks of the Andes and travel downstream to the coast at a decreasing gradient. As the rivers approach the coast, downstream "fining," or a decrease in the median particle size, occurs as a function of the decreasing sediment transport capacity (Parker 1991a, 1991b, 2008). Excess pore pressures that result in strength loss and deformations are sustained more easily in finer granular material due to its lower hydraulic conductivity than coarser granular material (Seed et al. 2003, Idriss and Boulanger 2007, Robertson 2010).

Transportation infrastructure, including bridges, roads, railroads, and other lifelines are particularly susceptible to damage when the soil liquefies. As such, the widespread liquefaction triggered during this event resulted in significant damage to several transportation structures. Although some of the observed damage was severe, the overall seismic performance of bridge decks and superstructures was quite good. The Ministry of Public Works (MOP, its Spanish acronym) reported that only 439 of 7,730 bridges, underpasses, and overpasses (i.e., 5.7%) suffered varying levels of earthquake-induced damage (MOP 2010). From a geotechnical point of view, the most commonly observed failure mechanism was shaking-induced settlement of fills. The second most common observation was the impact of liquefied

foundation soils on the deformation of approach fills at numerous bridge sites. Liquefaction and lateral spreading damaged many bridges, including the Mataquito, Rio Itata, Juan Pablo II, Llacolén, Bío-Bío, and Tubul bridges, as well as others.

Widespread damage also occurred in roads and railroads. Again, the most commonly observed geotechnical failure mechanism was shaking-induced settlement of compacted earth fills throughout the affected region. While there were isolated cases of embankment fill failures resulting in extended road closures (e.g., near Lota), most settlement-related damage to bridge approach fills and culvert backfills was quickly repaired using gravel "patches" to allow the roads to reopen quickly. While generally not a life-safety concern, these widespread fill settlements resulted in short-term traffic problems and high cumulative repair costs for the highway department. Geotechnical failure mechanisms commonly affecting railroads included shaking-induced slope failures, loss of rail alignment, and unseated railroad bridges. In most cases, the damage appeared to be limited and repairable, indicating good railroad performance despite the strong shaking that affected the region.

In this paper, selected bridge, road, and railroad damage cases investigated by the Geotechnical Extreme Events Reconnaissance (GEER) teams during several visits in 2010 are presented. Interested readers are referred to the GEER report edited by Bray and Frost (2010) for additional details of these and other cases related to the transportation infrastructure.

EFFECTS ON BRIDGES CROSSING THE BÍO-BÍO RIVER

The Bío-Bío River is the second longest river in Chile. It originates in the Andes and flows 380 km to the Gulf of Arauco on the Pacific Ocean. It is also the widest river in Chile, with an average width of 1 km, and a width of more than 2 km prior to discharging into the ocean. Close to the Pacific Ocean, the river traverses the metropolitan area of Concepción, Chile's second largest metropolitan area, which includes the cities of Talcahuano, San Pedro de la Paz, Lota, and Coronel. In Concepción, the river is crossed by five bridges (Figure 2): Llacolén Bridge (opened in 2000), Juan Pablo II Bridge (1973), La Mochita Bridge (2005), Puente Viejo Bridge (Old Bío-Bío Bridge, 1942) and Bío-Bío Railroad Bridge (1889). During the 27 February Maule earthquake, all of these bridges experienced different levels of structural damage, compromising normal business activities in the region. The most common geotechnical failure mechanism observed at these bridges was liquefaction-induced lateral spreading that occurred along both shores of the Bío-Bío River, which contributed to approach fill deformations. The most extensive lateral spreading-induced damage occurred at the Llacolén and Juan Pablo II bridges. Similarly, the La Mochita and Mataquito (near Iloca) Bridges were subjected to extensive lateral spreading effects, and their performance is also described herein.

LLACOLÉN BRIDGE

The Llacolén Bridge in Concepción was completed in 2000 and spans 2,160 m across the Bío-Bío River, supporting four lanes of vehicular, as well as pedestrian, access to downtown Concepción (Figures 2 and 3). During the earthquake, lateral spreading at the northeast approach unseated the bridge deck at its shoreline support (Figures 4 and 5), forcing closure of the bridge until a temporary deck could be erected (Figure 4). Ground damage at this approach was observed to extend inland into the southbound traffic

Figure 2. Aerial view of Concepción metropolitan area and Bío-Bío River main crossings.

Figure 3. Plan view of the Bío-Bío River region, locating the damaged region of the Llacolén Bridge in Concepción (S36.830108° W73.067991°).

lane of Calle Nueva road and continuing hundreds of meters northward and southward along a pedestrian walkway (Figure 5). Calle Nueva parallels the riverbank and runs under the bridge approach. Lateral spreading toward the river caused sufficient displacement to unseat the west and eastbound bridge deck (Figure 4). Closely spaced (0.1 m

Figure 4. Deck unseating at Llacolén Bridge in Concepción. Cracking resulting from lateral spreading is visible on right side of photo. View north (S36.830380° W73.067541°).

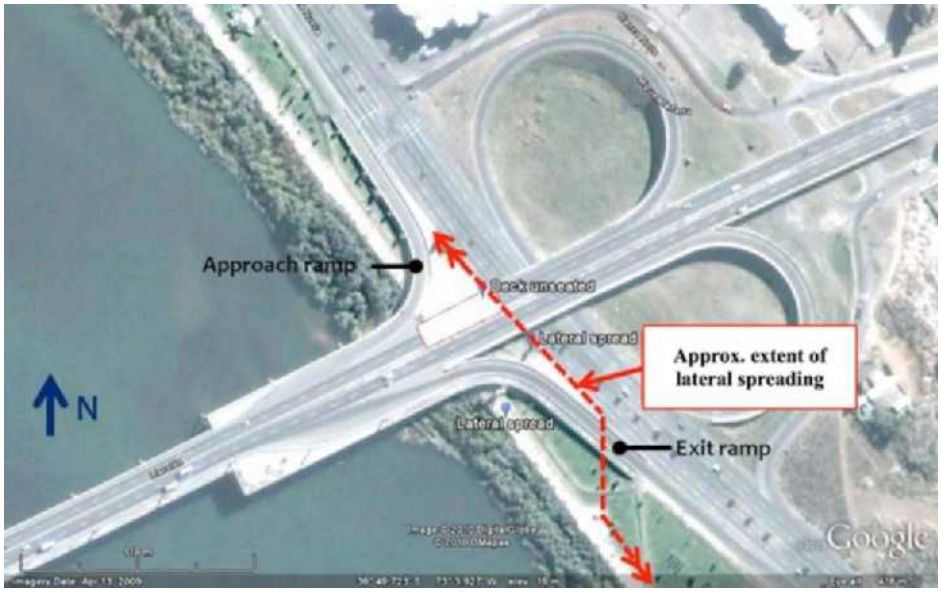

Figure 5. Plan view of the north approach to the damaged Llacolén Bridge in Concepción (S36.830108° W73.067991°).

to 0.2 m on center) flexural cracks on the riverside face of the 1.5 m diameter support columns were observed near the ground surface. The distribution of flexural cracking was more severe for those columns supporting the unseated deck; however, all columns at the north riverbank support experienced flexural cracking at their construction joint

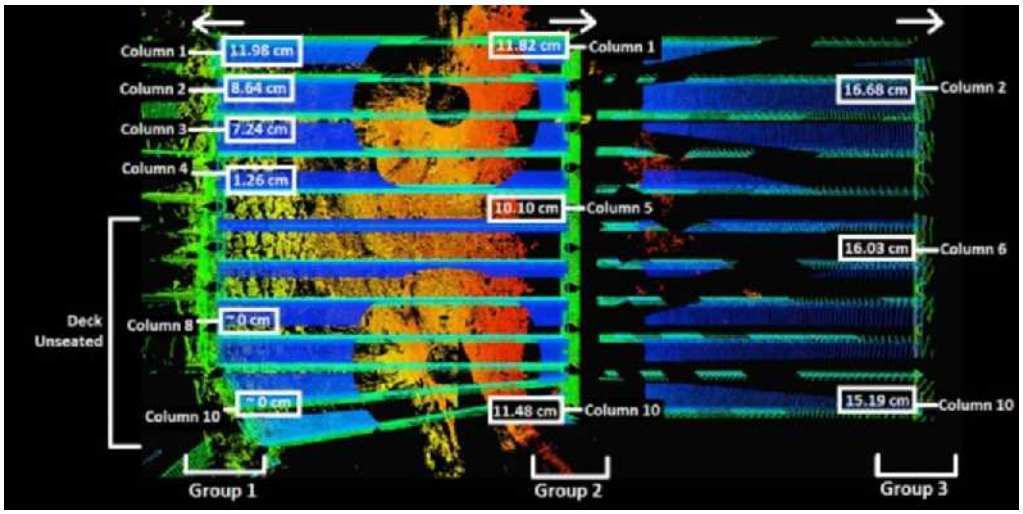

Figure 6. LIDAR measurements at the north end of Llacolén Bridge: Relative horizontal displacement of the columns with respect to their bases.

(between 2 m and 2.5 m above ground surface). Ground settlement of 0.25 m to 0.30 m also occurred at each of the exit ramp bents. According to FHWA (2011), the nearby ground settled up to 0.4 m and experienced significant shaking, resulting in a 0.25 m separation between the columns and the surrounding ground. Terrestrial LIDAR measurements, performed after the earthquake (Kayen 2012), show that the relative horizontal displacement of the columns with respect to their bases varied from 0 cm and 12 cm away from the river at the columns in the shoreline support, while the second and third rows of columns experienced a rather uniform displacement of their upper ends of 11 cm and 16 cm, respectively, toward the river (Figure 6).

As a measure of liquefaction susceptibility, the sand liquefaction triggering relationship of Youd et al. (2001) can be used to define a normalized SPT threshold value for the occurrence of liquefaction. The recorded peak ground accelerations in downtown Concepción were about 0.4g (Boroschek et al. 2010), and assuming that these soils may have a fines content on the order of 5% to 15%, an average stress reduction coefficient of about 0.9, a magnitude scaling factor of 0.75, and a σ_v/σ_v' ratio of about 2, the Youd et al. (2001) procedure estimates that sands with normalized SPT values below approximately 30 blows/foot were likely to liquefy during this event. Figure 7 shows that liquefiable soils were present along the Llacolén Bridge at many depths especially within the upper 3 m to 5 m. At the north approach, where earthquake-induced damage was concentrated, Boring S-6 indicates that liquefiable soils were present in the upper 8 m to 9 m of the soil deposit.

JUAN PABLO II BRIDGE

The Juan Pablo II Bridge is the longest vehicular bridge in Chile, spanning 2,310 m in length. This bridge, shown in Figure 8, connects the cities of Concepción and San Pedro de la

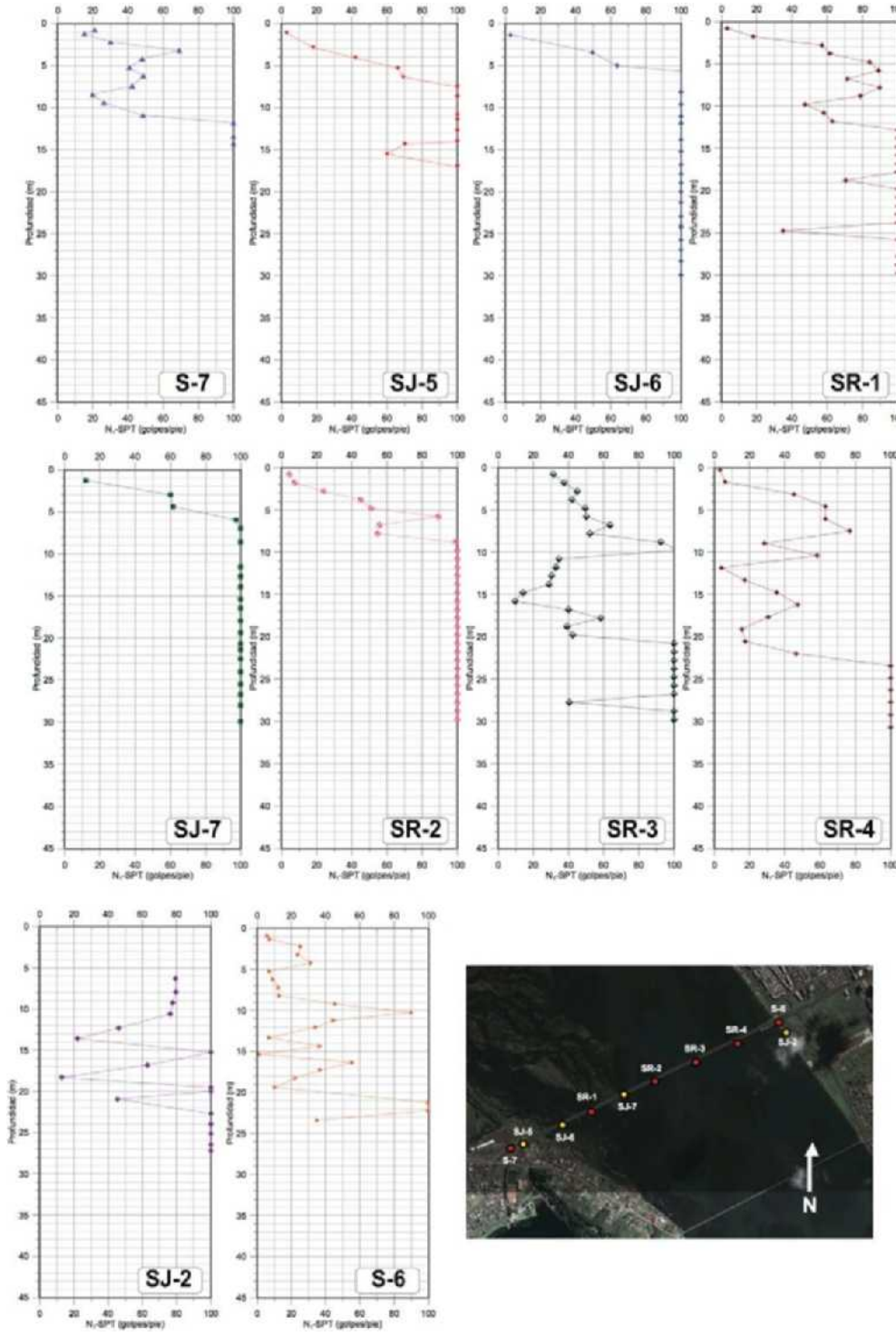

Figure 7. Normalized SPT values and boring locations at Llacolén Bridge. Pre-earthquake data (Verdugo and Peters 2010). "Profundidad (m) = Depth (m)," "(golpes/pie) = (blows/foot)."

Paz across the Bío-Bío River. The bridge opened to the public in 1974. The bridge consists of 70 spans (length = 33 m, width = 21.9 m), each composed of 7 reinforced concrete girders and a concrete deck. Each span sits on reinforced concrete bents with drilled pier supports (see Figure 8).

During the earthquake, the bridge suffered severe damage and was closed to the public. Liquefaction and lateral spreading at the northeast approach resulted in significant damage to the bridge superstructure (Figure 9). Most notably, liquefaction caused large settlements at several support piers and lateral displacement of the bridge deck. Visual inspection of the surrounding soils indicated the presence of fine loose sands. Several sand boil deposits with

Figure 8. Juan Pablo II Bridge connecting the cities of Concepción and San Pedro de la Paz across the Bío-Bío River. Typical bridge bent configuration shown in photograph inset.

Figure 9. Juan Pablo II northeast approach: (a) Settlement of bridge deck near bridge approach (view East, S36.815900° W73.084064°); (b) lateral spreading of northeast approach embankment.

diameters in the order of 1 to 10 meters were observed near the structure on both sides of the approach embankment.

Column shear failure, vertical displacements of the bridge deck of up to 1 m, and rotation of the bridge bent of 1° to 3° occurred at the northeast approach. Figure 10 shows the shear failure of the column facing the bent's south side. The north column, also shown in Figure 10,

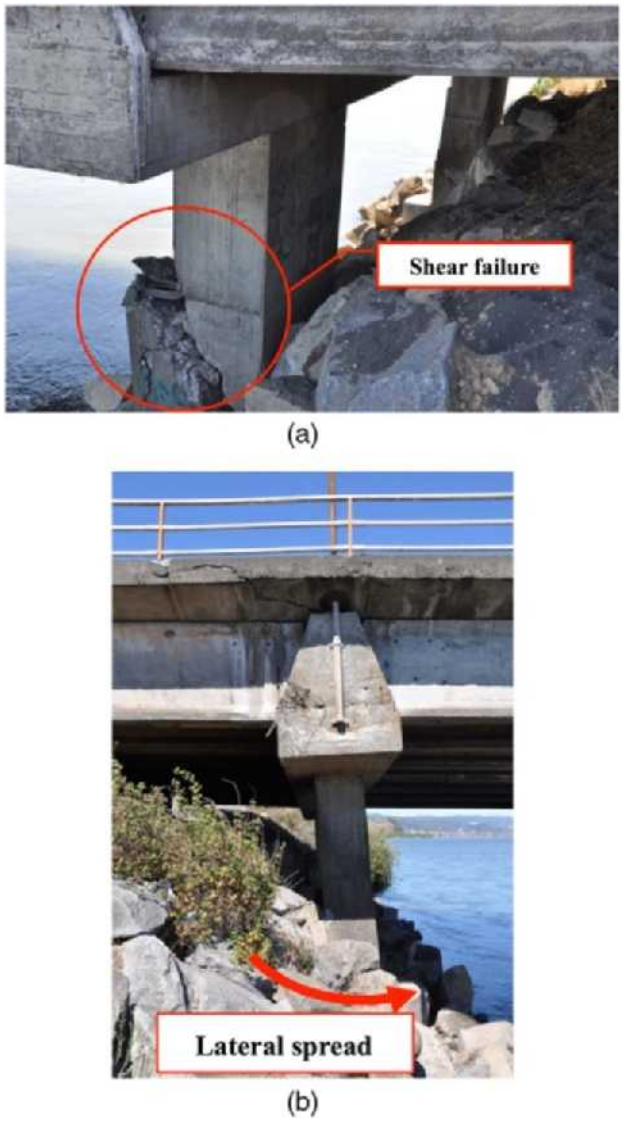

Figure 10. Juan Pablo II Bridge northeast approach: (a) Column shear failure, looking west, S36.816233° W73.084144°; and (b) rotation and lateral displacement of bridge bent, looking east, S36.816233° W73.084144°.

exhibited tension cracks and rotation as well as shear failure. In contrast with the damage observed at the northeast approach, the southwest approach suffered minor damage. This may be due to a combination of different soils conditions and more gentle slopes observed at the southwest approach.

Pier settlements of 0.4 m to 1.5 m were observed at several locations along the length of the bridge (Figure 11). Vertical settlements appeared to be due to liquefaction of the soil near the pier foundations. Short pier foundation depths on the order of 16 m (in contrast to 22 m for the Llacolén Bridge) may also have contributed to these settlements. Visual inspection of the surrounding soils indicated the presence of loose sands near the surface. Although the Bío-Bío River was once navigable by ship up to the City of Nacimiento, over-logging during the twentieth century led to heavy erosion, choking the river with silt, and rendering it impassable to ship traffic. Near Concepción, the river behaves as a meandering river with fine-grained material deposited on the floodplains.

Settlements on the order of 0.6 m to 0.8 m were observed in piers #45 and #60, as indicated in Figures 11 and 12. The bridge deck accommodated these settlements with large vertical deformations, however relatively minor damage of the asphaltic layer was observed. As Figure 12 shows, settlements of piers #45 and #65 were larger on the upstream side, indicating rotation of these bents about the longitudinal axis of the bridge. This is consistent with the observations made by FHWA (2011): "... the spans of the main bridge also appeared to have experienced uneven support settlement, which tilted the columns and rotated the bridge deck about the centerline of the bridge." Soil in the vicinity of the

Figure 11. Juan Pablo II Bridge. Pier settlements (Pier #0 corresponds to San Pedro end).

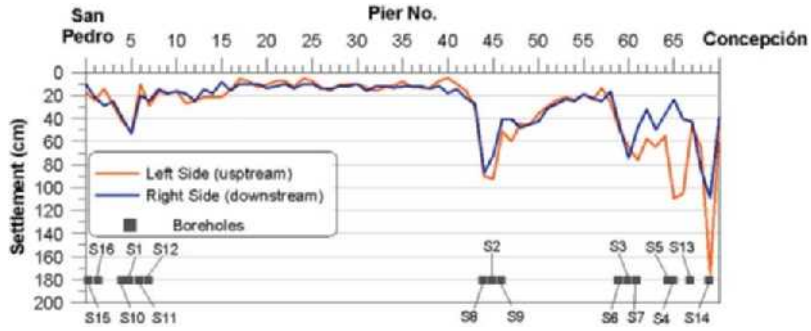

Figure 12. Juan Pablo II Bridge. Pier settlements and boring locations (Verdugo and Peters 2010).

piers showed evidence of ejected water and sand, while soil immediately surrounding the pier was depressed with standing water covering an annular zone around the pier. These observations are supported by the SPT profiles obtained after the earthquake along the bridge, shown in Figure 13, where the white color corresponds to non-liquefiable sands, green is for soils with a high content of non-plastic silts (termed as "non-liquefiable" in the report), and red is for liquefiable sands, according to the criteria used by Verdugo and Peters (2010) in their geotechnical report. Using the 30 blows/foot criterion discussed in the previous section, distinct layers of liquefiable material can be observed on the geotechnical cross-section along the Juan Pablo II Bridge.

LA MOCHITA BRIDGE

The La Mochita Bridge, shown in Figure 14, is a four-span (15, 50, 50, and 35 m spans) concrete bridge supported by seat-type abutments at each end and two-column bents at the interior locations. At this site, ground failure occurred along the NW–SE trending spit inducing transverse movement of the bridge superstructure. The transverse nature of ground failure observed at this bridge is unique compared to other failures observed elsewhere in Concepción and during past earthquakes, where lateral spreading or other ground failure typically causes bridge movement in the direction of the longitudinal axis of the bridge.

This bridge, which was completed in 2005, spans north–south along the east bank of the Bío-Bío River, crossing a small inlet of water that fronts a water treatment facility in south Concepción. Bents are comprised of two 1.5 m diameter concrete columns with pin connections at the deck, which are restrained vertically with a pair of tie bars integrated with a concrete block assembly (vertical restrainer blocks). The column bases are integrated with a concrete cap embedded below the ground. The bridge superstructure is composed of precast I-girders and a concrete slab. Bents #2 and #3 are founded on a soil spit that slopes toward the east water inlet. The highest elevation of the soil spit is approximately 6 to 10 m east of the Bío-Bío River. At the time of the GEER team visits, the river was low enough that the base of the pile caps was visible.

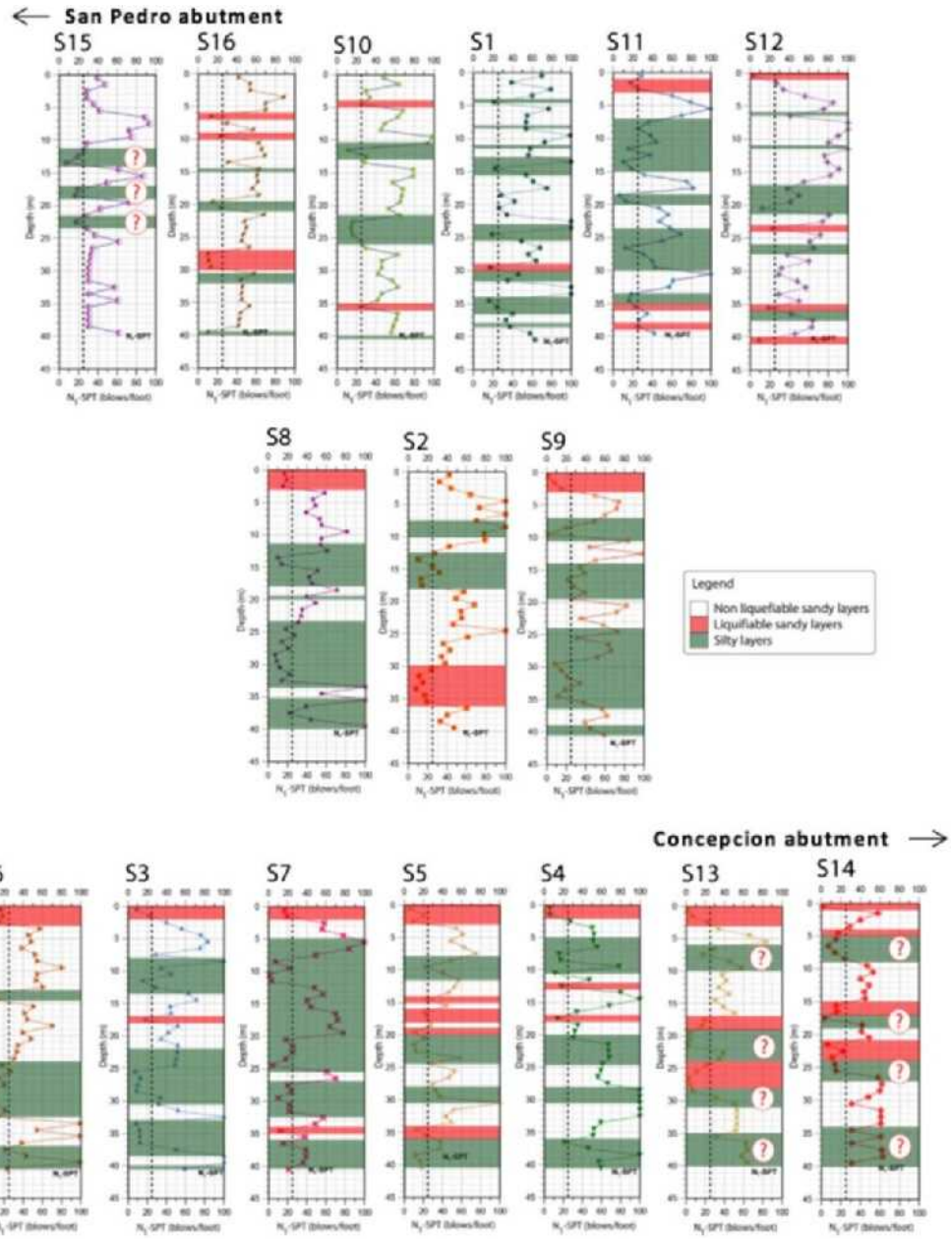

Figure 13. Normalized SPT values at Juan Pablo II Bridge (post-earthquake data). White is for non-liquefiable sands, green is for silty soils (mainly non-plastic silts), and red is for liquefiable sands (Verdugo and Peters 2010).

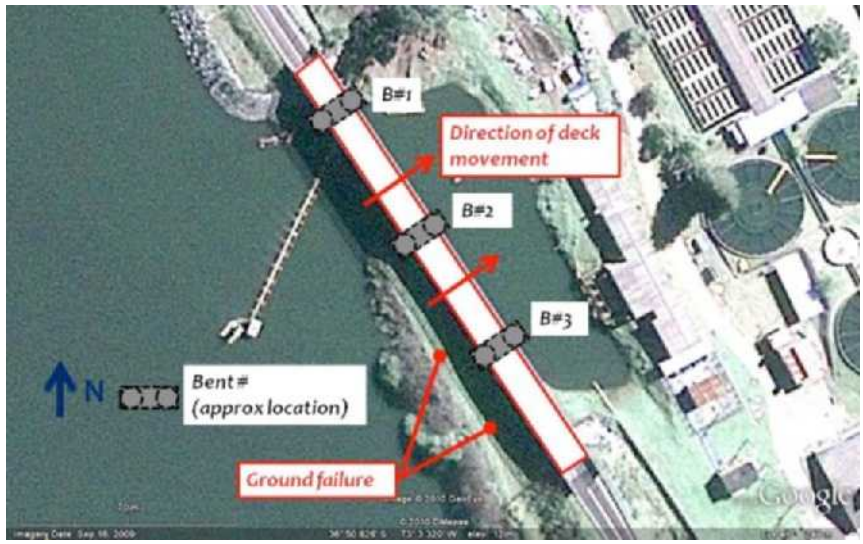

Figure 14. Plan view of the La Mochita Bridge in south Concepción describing observed damage (S36.846841° W73.055496°).

The bridge superstructure shifted transversely, largely as a unit, toward the east due to failure of the soil spit (Figure 16a). This failure may be attributable to either a deep-seated slope instability or a liquefaction-induced lateral spreading mechanism. The SPT profiles from the original project (Figure 15) show that the deep-seated slope instability is a possible mechanism of failure (note how the SPT values drop at depths of 15 m to 20 m). However, sand boils below the bridge were observed near bents #2 and #3 (Figure 16b), and the transverse rotation, or vertical movement, of the bents was limited, which suggests that liquefaction-induced lateral spreading could have also played a role in the bridge failure.

Measurements taken by the team on 15 March 2010, indicated that the north end of the bridge deck shifted 0.5 m to the east relative to the approach fill, while the south end of the bridge shifted 0.9 m toward the east relative to the approach fill on that side. LIDAR measurements show that these lateral displacements were, respectively, 0.3 m and 0.8 m (Kayen 2012). Bents #2 and #3 subassemblies (columns, bent cap, and pile cap) were observed to rotate slightly about the longitudinal axis of the bridge toward the east consistent with the deck movement. Rotations of bents #2 and #3 were measured as 2º and 4º, respectively. Bent #1 could not be accessed at the time of the teams' visit; however, views from the spit suggested that the deck moved independently of bent #1. Movement of the abutments was observed to be minimal, with the resulting damage to the superstructure largely attributed to the translation of the bents (Figure 16c). FHWA (2011) indicates that fill settlement at the abutments varied from 0.3 m to 0.8 m, and that the piers moved laterally about 0.1 m to 0.15 m, and vertically about 0.05 m to 0.1 m. It is noted that movement of the bridge, either shaking- or kinematically-induced, resulted in damage to both east and west end transverse shear keys of the interior bents (Figure 16d).

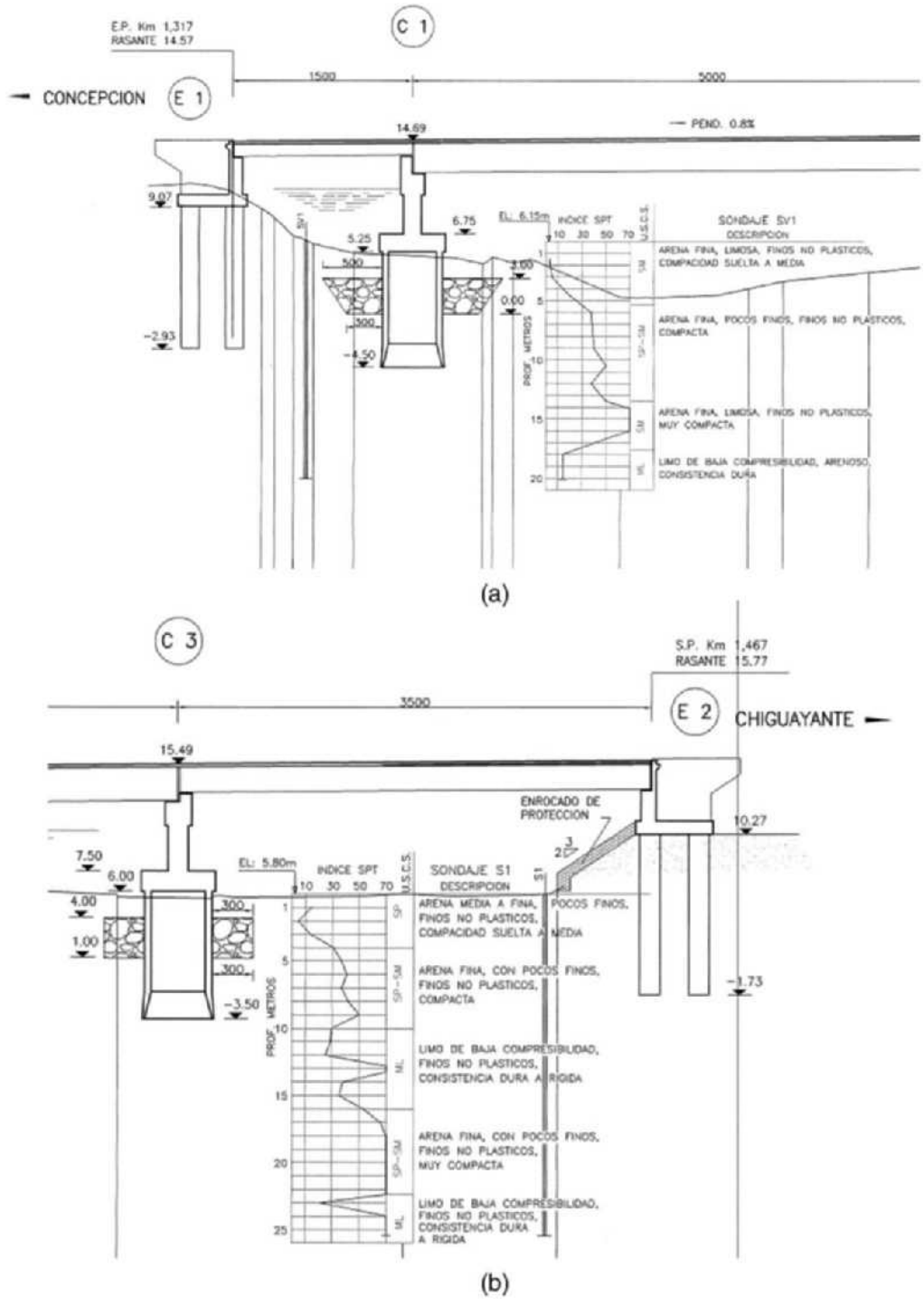

Figure 15. SPT profiles at both ends of La Mochita Bridge (pre-earthquake data): (a) Concepción abutment and (b) Chiguayante abutment (MOP 2010).

Figure 16. Liquefaction-induced damage at La Mochita bridge: (a) Looking north at bent #3, S36.847389° W73.055219°; (b) sand boils observed below the bridge, S36.847456° W73.055129°; (c) transverse shift of deck relative to south abutment, S36.847547° W73.054876°; and (d) damage to transverse shear key at bent #3, S36.847405° W73.055084°.

MATAQUITO BRIDGE

The Mataquito Bridge is a 320 m-long, eight-span, reinforced concrete structure that crosses the Mataquito River close to the Pacific Ocean. Each pier of this bridge consists of three columns of circular section. This bridge experienced liquefaction under the approach fills that contributed to deformations (Figure 17). The north approach was founded on alluvial sediments that liquefied and spread toward the river, causing moderate to significant transverse and longitudinal deformations in the approach fill. In contrast, the south approach was founded on dune sands over possibly shallow bedrock and exhibited negligible deformations. Lateral spreading occurred near both north and south bridge bents, but the deformations appear to have been limited by the "pinning" effect from the pile foundations, as the lateral deformation of the ground behind the bridge foundation was essentially zero, while just outside the pile caps these deformations were in the order of 1 m to 2 m. Despite evidence of liquefaction at both abutments of the bridge, its structure remained undamaged and functional, and the residual displacements of the bridge foundations were insignificant.

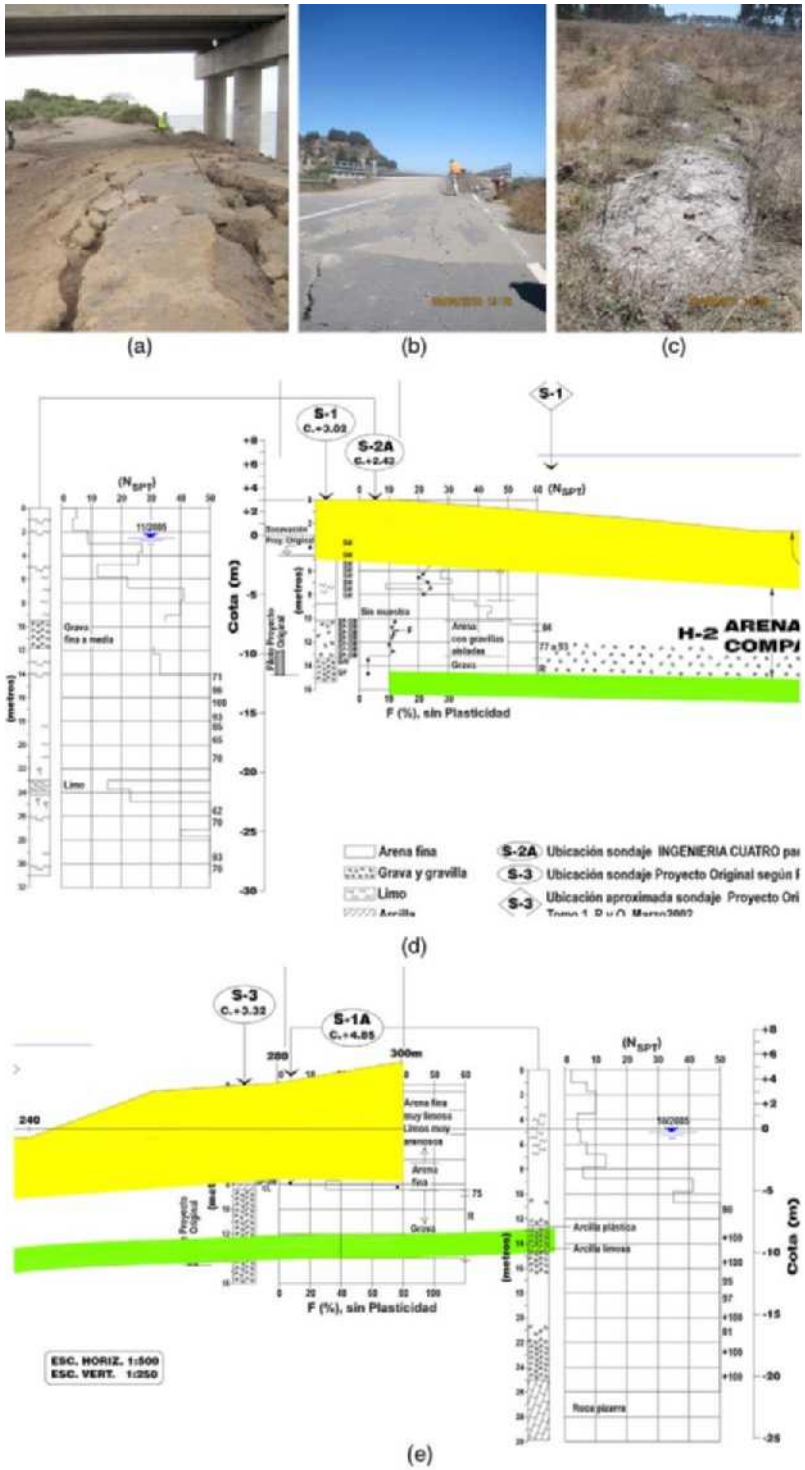

Figure 17. Mataquito bridge: (a) Lateral spreading on the south end of the bridge, S35.050712° W72.162258°; (b) approach fill settlement at the north abutment of the bridge (70 cm offset at the bridge deck), S35.050712° W72.162258°; (c) sand boils at the north end, S35.051961° W72.163217°; (d) SPT profiles at the Iloca (north) abutment; and (e) SPT profiles at the Quivolgo (south) abutment. Colors in (d) and (e) represent different soil units. SPT profiles obtained before the earthquake.

Soil conditions at the north (Iloca) abutment consist of 5 m of liquefiable fine sand with SPT values ranging from 5 to 20 blows/foot, underlain by a layer of fine compact sand 9 m thick, which in turn is underlain by sandy gravel (Figure 17d). Soil conditions at the south (Quivolgo) abutment consist of 9 m of liquefiable fine sand with SPT values below 10 blows/foot, underlain by a layer of fine compact sand 4 m thick, which in turn is underlain by sandy gravel (Figure 17e).

Lateral spreading on the south abutment appeared to be more confined, probably due to a combination of the topography of the area and the "pile-pinning" effect. In contrast, on the north side, and due to the large extent of the fields that surround the bridge, moderate to significant lateral spreading was observed extending landward 270 m from the river edge. Lateral spreading from the edge of the abutment wall to the first row of piers was about 54 cm and the total lateral spreading from the edge of the abutment wall to the river's edge was about 180 cm (over a distance of about 65 m). The approach embankment is about 7.6 m high, and settled about 70 cm relative to the bridge deck. The approach embankment experienced a transverse movement of about 60 cm from the centerline as manifested by cracking of the asphalt over a distance of about 200 m. The locally heaved ground, observed at the toe of the embankment, indicates soil crust compression, likely as a result of liquefaction of the underlying soil. A bridge girder was partially sheared at the first pier on the north side. The bridge remained in use after the earthquake.

EFFECTS ON ROADS

The Pan American Highway (Ruta 5) runs north–south and crosses many rivers, waterways, canals, and ditches in the central region of Chile. The central region is an agricultural region with east–west trending drainages spaced at 30–50 km. Surface evidence of liquefaction was observed and deformations impacted some bridge approach fills. The most frequent damage along Ruta 5 occurred at relatively unengineered water crossings, such as canals and ditches. Systematic failures also occurred where culverts, box sections, and other minor water conduits intersected the highway. Generally, engineered river crossings performed adequately during the earthquake.

TWO SIGNIFICANT ROAD EMBANKMENT FAILURES ALONG ROUTE 5

Two collapsed embankment fills were identified near Copihue and Parral. The first, shown in Figure 18, occurred along a straight section of Ruta 5 located approximately 8 km north of Parral. The southbound lanes collapsed to the west, apparently as a result of a shallow translational slide in near-surface foundation soils (~ lateral spreading), as evidenced by the failed soil mass location and a mound of soil pushed up at the west toe of the embankment (Figure 18a). The embankment failed along a length of approximately 150 m at a location where a low-lying softer soil was located at the toe. No geotechnical information could be found for this specific location. However, the soil conditions nearby consist of about 4 m of sandy silt and silty clay (SPT values below 20 blows/foot) underlain by cemented sandy silt, locally known as "tosca." Geotechnical information found for this area shows that the location of the phreatic surface varies seasonally from 1 m to 9 m deep (Figure 19).

The second failure (Figure 20) occurred on an overpass of Ruta 5 located approximately 13 km north of Parral. The overpass embankment was curved and the embankment failed

Figure 18. Embankment fill collapsed near Copihue, north of Parral, closing the southbound lanes of Ruta 5: (a) view from the south, (b) view from the north, S36.087891° W71.791513°.

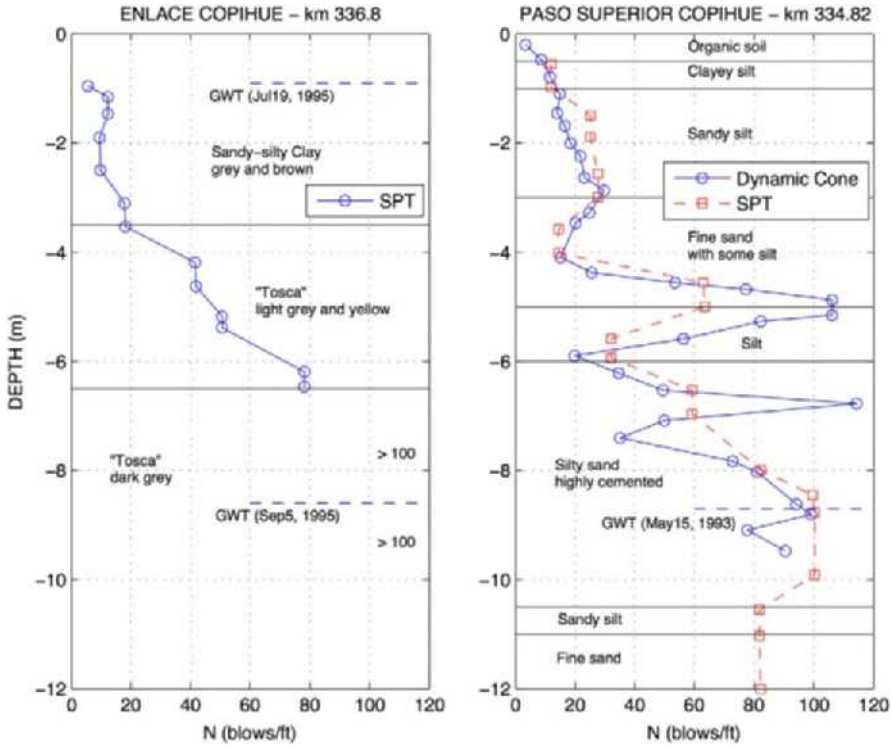

Figure 19. SPT and DCPT data in the Copihue area (adapted from MOP 2010). Pre-earthquake data.

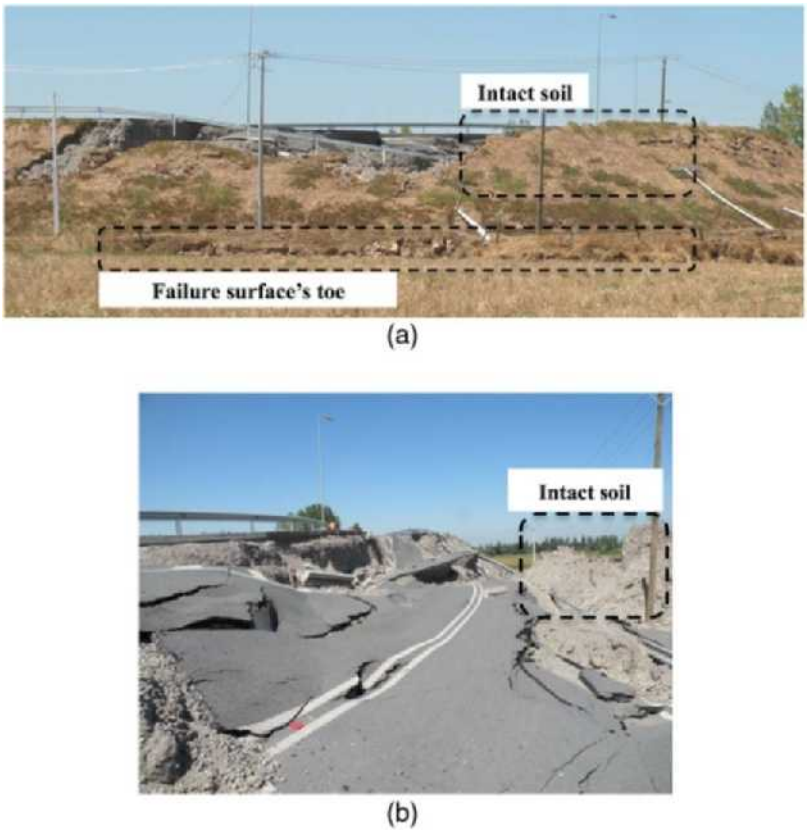

Figure 20. Curved overpass embankment failure 13 km North of Parral: (a) Translational 3D slide failure, S36.0343° W71.7568°; and (b) failed outside of the curved embankment, S36.0347° W71.7558°.

over a length of about 80 m toward the outside of the curved section. Again, the failure appeared to involve a shallow translational slide in the near surface foundation soils, as evidenced by the intact failed soil mass and the mound of soil pushed up at the toe (Figure 20). Three-dimensional effects potentially contributed to failure to the outside of the curved embankment section as opposed to the inside of the embankment. As Figure 20 shows, a portion of the outside section of the slide mass displaced laterally about 6 m (Kayen 2012), and it remained completely intact.

ROAD EMBANKMENT FAILURES NORTH OF LOTA

Several large ground failure areas were observed north of Lota along Route 160. Two failures resulted in damage to a roadway embankment section (denoted herein as the "southbound failure" and "northbound failure" in Figures 21 and 22, respectively), while a third failure resulted in damage to an elevated railroad section (denoted as "railroad failure" and discussed in the subsequent section). Minor side road spreading failures were also observed

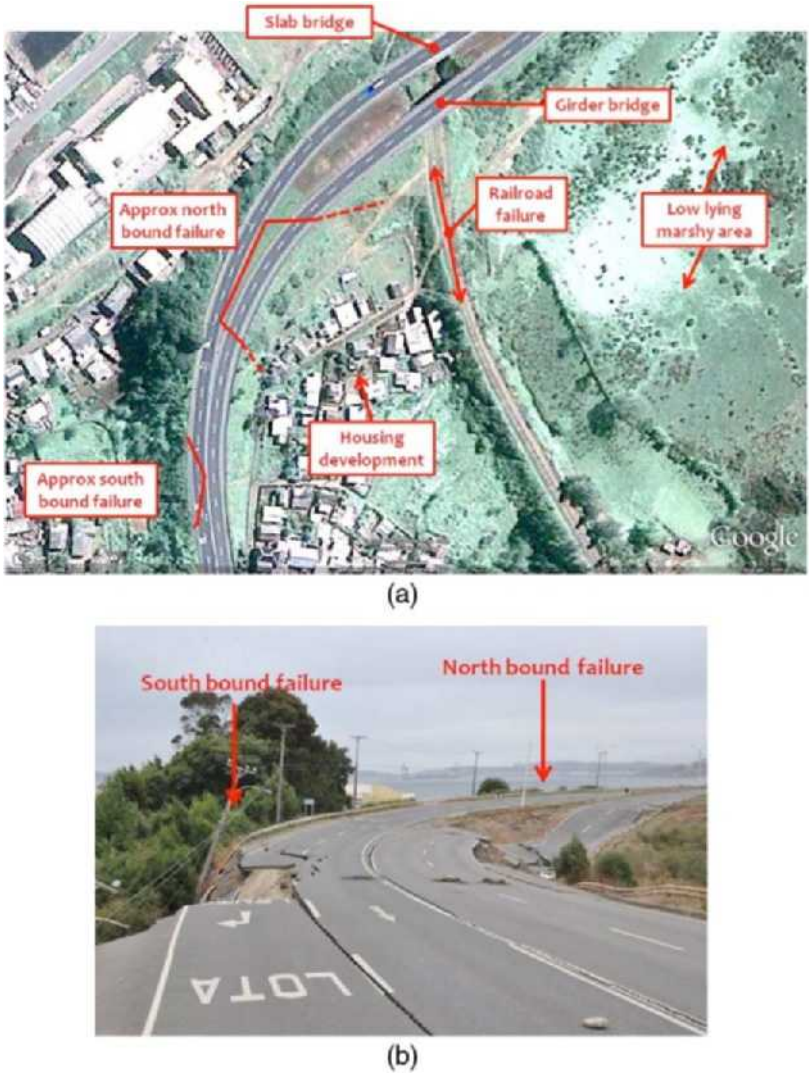

Figure 21. (a) Plan view of approximate affected area, S37.0734° W73.1469°; and (b) view looking north on Route 160 showing south bound and north bound failure areas, S37.0744° W73.1480°.

near the approaches to two short-span overpass bridges, north of the embankment failures, as well as just north of the short span bridges. The area east of Route 160 is largely a low-lying marsh (Figure 21a). South of the northbound failure and east of the southbound failure of the elevated roadway sections there is a small housing development.

The northbound slope failure appeared to be deeply seated, perhaps due to softening of the foundation materials. It was not clear whether the southbound failure was due to a deep-seated foundation failure or due to poorly compacted earth fill in the embankment section.

Figure 22. (a) View looking south on route 160 showing north bound failure area, S37.0730° W73.1475°; and (b) view looking north showing south bound failure area, S37.0746° W73.1479°.

LIDAR measurements (Kayen 2012) indicate that the maximum lateral and vertical displacements of the failed paved road were, 6.1 m and 7.1 m respectively, for the northbound failure, and 4.9 m and 7.3 m respectively, for the southbound failure. A gray sandy fill overlaid by compacted clay fill was used in the elevated road embankment. The roadway elevation was approximately 10 m to 15 m above the valley area (10 m nearest to the overcrossing bridges, with a high point adjacent to the housing development area).

EFFECTS ON RAILROADS

RAILROAD BRIDGE OVER THE BÍO-BÍO RIVER

The Bío-Bío River railroad bridge is one of the oldest crossings of the Bío-Bío River. Originally built in 1889, it was retrofitted completely in 2005. This railroad structure is composed of parallel top and bottom chords separated by diagonal and vertical members in a Warren truss arrangement. Three hundred seventy pillars support the structure, covering a length of 1,889 m. The bridge was damaged during the earthquake by strong shaking and possibly lateral spreading of the riverbanks. This damage included several broken bracing rods, at least two fractured steel piles, displaced steel tubes, and a displaced retaining wall (FHWA 2011). Of the 370 pillars of the bridge, 19 were damaged during the earthquake, and several portions of the rail were bent or misaligned (Figure 23). Visual inspection of pillars near the west abutment indicates that several piles translated laterally and rotated (Figure 24). The rail lines were moved out of alignment, as shown in Figure 23b. FHWA (2011) indicates that the shoreline pier's lateral displacement toward the river was 0.7 m and that the ground around the pier settled 1.3 m.

RAILROAD EMBANKMENT FAILURES NORTH OF LOTA

The bridge overcrossings, and therefore the road embankments, of the north- and southbound sections of Highway 160 north of Lota may have been constructed at different times, as evidenced by differences in construction type of the bridges (Figure 25a; also, see

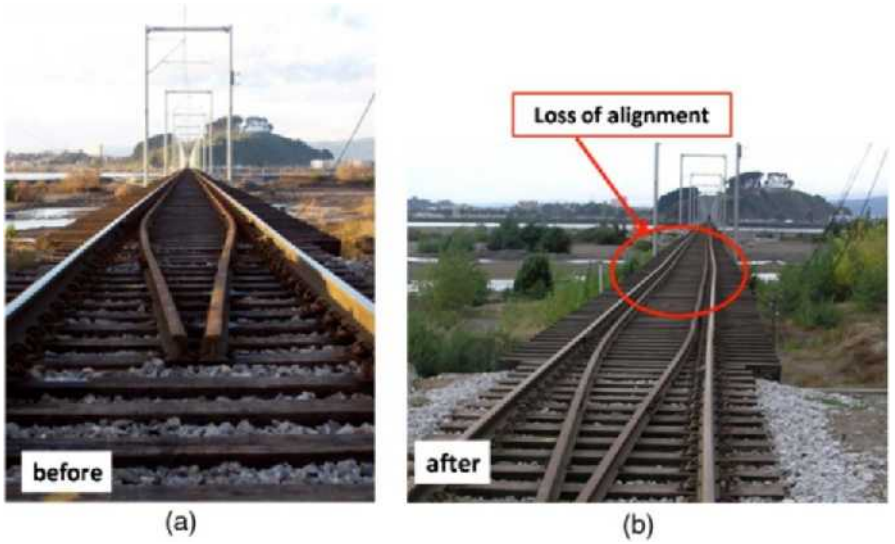

Figure 23. (a) Rails aligned before earthquake and (b) rails bent after earthquake, S36.836097° W73.087094°.

Figure 24. Bío-Bío River railroad bridge: (a) Pillars translated and rotated during earthquake; (b) detail of broken crossbar, S36.836075° W73.086969°.

Figure 21a, denoted as slab and girder bridges). The neighboring elevated railroad failure is characterized as a slump with lateral spreading, likely due to settlement of the compacted fill (Figure 25a). The railroad was approximately 5 m to 7 m above the low-lying marshy area along the section that failed.

Figure 25. (a) Slab and girder-type overpasses at northern end of road embankment failure area, showing railroad and supporting ground settlement (view looking west), S37.0729° W73.1469°; and (b) ground failure below elevated railroad east of road embankment failure (view looking east), S37.0727° W73.1471°.

CONCLUSIONS

Liquefaction was widespread throughout the region subjected to strong ground motions during the 2010 Maule, Chile, earthquake. Liquefaction occurred primarily in sandy deposits along the rivers that run in the east–west direction across central Chile. Liquefaction of these soils resulted in moderate-to-severe damage to many bridges, railroads, highways, and other lifelines. While the damage resulting from the earthquake-induced tsunami was more severe than that resulting from liquefaction, the cost of repairing damaged infrastructure will be very high because of how widespread the liquefaction damage was. Specific performance examples of bridges, railroads, highways, embankments, and other lifelines were presented in this paper. One of the notable failures was that of La Mochita Bridge, which involved significant transverse displacement of the bridge as a result of a unique lateral spread. Transverse bridge displacement represents an important case history because this mode of failure has not been previously observed. The deformation pattern that was observed at Juan Pablo II Bridge's river piers is also interesting. In this case, liquefaction of a finite number of soil layers bounded by non-liquefiable material induced large vertical settlements, as large as 0.8 m in some cases, with almost no evidence of lateral displacements.

ACKNOWLEDGMENTS

This material is based upon work supported by the National Science Foundation (NSF) under Grant No. CMMI-1034831. Any opinions, findings, and conclusions or recommendations expressed in this material are those of the authors and do not necessarily reflect the views of the NSF. Additional support was provided by Golder Associates and

the Chilean Air Force. All GEER team members contributed to this effort, including Jonathan Bray, David Frost, Ramon Verdugo, Christian Ledezma, Terry Eldridge, Pedro Arduino, Scott Ashford, Dominic Assimaki, David Baska, Jim Bay, R. Boroschek, Gabriel Candia, Leonardo Dorador, Aldo Faúndez, Gabriel Ferrer, Lenart Gonzalez, Youssef Hashash, Tara Hutchinson, Laurie Johnson, Katherine Jones, Keith Kelson, Rob Kayen, Gonzalo Montalva, Robb Moss, Sebastian Maureira, George Mylonakis, Scott Olson, Kyle Rollins, Nicholas Sitar, Jonathan Stewart, Mesut Turel, Alfredo Urzúa, Claudia Welker, and Rob Witter.

REFERENCES

Boroschek, R., Soto, P., and León, R., 2010. *Registros del Terremoto del Maule, $M_w = 8.8$, 27 de Febrero de 2010*, RENADIC Report 10/05, August 2010.

Bray, J. D., and Frost, J. D., Eds., 2010. *Geo-engineering Reconnaissance of the 2010 Maule, Chile, Earthquake, a Report of the NSF- Sponsored GEER Association Team*, primary authors: Arduino et al., http://www.geerassociation.org/.

Federal Highway Administration (FHWA), 2011. *Post-Earthquake Reconnaissance Report on Transportation Infrastructure: Impact of the 27 February 2010, Offshore Maule Earthquake in Chile*. Authors: Wen-Huei Phillip Yen, Genda Chen, Ian Buckle, Tony Allen, Daniel Alzamora, Jeffrey Ger, and Juan G. Arias. Report No. FHWA-HRT-11-030, March 2011.

Idriss, I. M., and Boulanger, R. W., 2007. SPT- and CPT-based relationships for the residual shear strength of liquefied soils, *4th International Conference on Earthquake Geotechnical Engineering—Invited Lectures*, K. D. Pitilakis, ed., Springer, The Netherlands, 1–22.

Kayen, R., 2012. Personal communication.

Ministerio de Obras Públicas (MOP), 2010. Personal communication.

Parker, G., 1991a. Selective sorting and abrasion of river gravel I: Theory, *ASCE Journal of Hydraulic Engineering* **117**, 131–149.

Parker, G., 1991b. Selective sorting and abrasion of river gravel II: Applications, *ASCE Journal of Hydraulic Engineering* **117**, 150–171.

Parker, G., 2008. Transport of gravel and sediment mixtures, in *Sedimentation Engineering: Processes, Measurements, Modeling, and Practice, Manual No. 110*, M. Garcia, ed., ASCE, Reston, VA.

Robertson, P. K., 2010. Evaluation of flow liquefaction and liquefied strength using the cone penetration test, *J. Geotech. Geoenviron. Eng.* **136**, 842–853.

Seed, R. B., Cetin, K. O., Moss, R. E. S., Kammerer, A., Wu, J., Pestana, J., Riemer, M., Sancio, R. B., Bray, J. D., Kayen, R. E., and Faris, A., 2003. *Recent Advances in Soil Liquefaction Engineering: A Unified and Consistent Framework*, Earthquake Engineering Research Center Report No. EERC 2003-06. http://eerc.berkeley.edu/reports/.

United States Geological Survey (USGS) 2010. *Pager—M8.8 Offshore Maule, Chile, Estimated Modified Mercalli Intensity*, http://earthquake.usgs.gov/earthquakes/pager/events/us/2010tfan/index.html

Verdugo, R., and Peters, G., 2010. *Informe Geotécnico Fase Anteproyecto Infraestructura Puente Mecano Eje Chacabuco*, Rev7, August 2010.

Verdugo, R., 2011. Personal communication.

Youd, T. L., Idriss, I. M., Andrus, R. D., Arango, I., Castro, G., Christian, J. T., Dobry, R., Finn, L., Harder Jr., L. F., Hynes, M. E., Ishihara, K., Koester, J. P., Liao, S. C., Marcuson III, W. F., Martin, G. R., Mitchell, J. K., Moriwaki, Y., Power, M. S., Robertson, P. K., Seed, R. B., and Stokoe II, K. H., 2001. Liquefaction resistance of soils: Summary report from the 1996 NCEER and 1998 NCEER/NSF workshops on evaluation of liquefaction resistance of soils, *Journal of Geotechnical and Geoenvironmental Engineering*, ASCE **127**, 817–833.

(Received 15 March 2011; accepted 19 February 2012)